Electromigration Study in SnAg3.8Cu0.7 Solder Joints on Ti/Cr-Cu/Cu Under-Bump Metallization

YING-CHAO HSU,[1] TUNG-LIANG SHAO,[1] CHING-JUNG YANG,[1] and CHIH CHEN[1,2]

1.—Department of Materials Science and Engineering, National Chiao Tung University, Hsin-Chu, Taiwan 300, Republic of China. 2.—E-mail: vins@ms8.hinet.net

This paper investigates the electromigration-induced failures of SnAg3.8Cu0.7 flip-chip solder joints. An under-bump metallization (UBM) of a Ti/Cr-Cu/Cu trilayer was deposited on the chip side, and a Cu/Ni(P)/Au pad was deposited on the BT board side. Electromigration damages were observed in the bumps under a current density of 2×10^4 A/cm^2 and 1×10^4 A/cm^2 at 100°C and 150°C. The failures were found to be at the cathode/chip side, and the current crowding effect played an important role in the failures. Copper atoms were found to move in the direction of the electron flow to form intermetallic compounds (IMCs) at the interface of solder and pad metallization as a result of current stressing.

Key words: Electromigration, flip chip, under-bump metallization, BT board, current crowding, intermetallic compounds

INTRODUCTION

Flip-chip technology is used widely in the modern electronics industry because of the higher packaging density (more inputs/outputs), better performances, smaller device footprints, and lower packaging profiles. As the number of input/output pin counts increase for the flip-chip products in the near future, the bump pitch and the diameter of under-bump metallization (UBM) will decrease accordingly because of the small contact area of the solder bumps. The size of solder bumps in flip-chip technology is approaching 50 μm in diameter. If a solder bump is to carry a 0.2-A electrical current, its current density will reach 10^4 A/cm^2. The current density is large enough to cause electromigration damage. Therefore, the electromigration in flip-chip solder bumps needs to be investigated urgently.[1–3]

Recent studies on electromigration in solder materials mainly focus on electric current effects upon interfacial reactions and the eutectic SnPb solder.[4–11] Because of the heightened awareness of environmental concerns, Pb-containing solders will be replaced by Pb-free solders. The SnAg3.8Cu0.7 solder will be one of the most promising lead-free solders for the microelectronic packaging industry. However, little research has been done on the electromigration of SnAg3.8Cu0.7 solder bonded to Ti/Cr-Cu/Cu thin-film UBM.[12–14]

This study examines the electromigration damage in flip-chip SnAg3.8Cu0.7 bumps on Ti/Cr-Cu/Cu UBM under the current density of 2×10^4 A/cm^2 and 1×10^4 A/cm^{2}at 100°C and 150°C. Current crowding[15–19] and polarity effect are also investigated, and the possible failure mechanism will be discussed in this paper.

EXPERIMENTAL PROCEDURE

A UBM of a Ti/Cr-Cu/Cu trilayer was deposited on the chip side, and a Cu/Ni(P)/Au pad was electroless plated on the BT board side. The solder bumps on the chip were formed by printing solder paste through a metal stencil and were reflowed in a furnace at 250°C. The chips were then flipped over, aligned to BT substrates, and reflowed again. The reflow profile of the solder bumps is presented in Fig. 1. Afterward, the package was filled with underfill. The solder bumps were electrically connected by an Al line in the chip, while a Cu line was used in the BT board side. A schematic illustration of the structure is shown in Fig. 2a, which shows that the contact window in the chip side was 85 μm and 150

(Received March 4, 2003; accepted May 15, 2003)

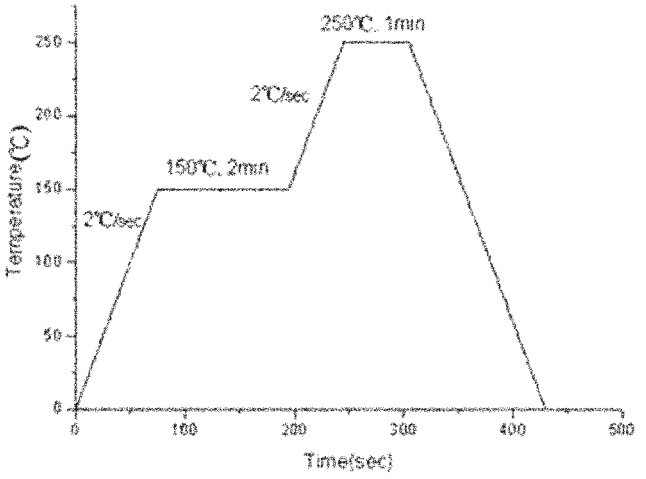

Fig. 1. The reflow profile for the solder bumps.

μm for board side. The pitch for the sample was 400 μm. Figure 2b is a three-dimensional schematic diagram of the bump pairs subjected to electromigration testing in which the routes for the electrical current are depicted. Two sets of bump pairs, Pair A and Pair B, were employed for electromigration study. The current paths for bump Pair A and Pair B are indicated by the arrows in Fig. 2b.

Cross-sectioned bumps and whole-bump samples were prepared for the electromigration test. Cross-sectioned bumps refer to those bumps that had been cross-sectioned first and then stressed. To investigate the current crowding effect, two different cross sections, i.e., cross-section A and cross-section B, were prepared, as shown schematically in Fig. 2c. The samples were stressed at 100°C or 150°C on a hot plate in ordinary atmospheric conditions. The calculated current density was 2×10^4 A/cm^2 for the contact opening on the chip side and 6.6×10^3 A/cm^2 for the contact opening on the board side. Resistance change caused by electromigration was monitored every 10 sec during the current stressing. Electromigration damage was examined using a scanning electron microscope (SEM). Energy dispersive spectroscopy (EDS) was used to determine the composition of intermetallic compounds (IMCs) and the distribution of metal atoms.

RESULTS

Composition and Microstructure of the Intermetallic Compound before Current Stressing

Figure 3a illustrates the cross-sectional SEM image of the SnAgCu solder bump before current stressing. In the bulk solder, the composition of the IMC was identified to be Cu_6Sn_5 with dissolution of 2–4 at.% of Ni. The Ag_3Sn particles were also found in the solder bump. Figure 3b and c shows the

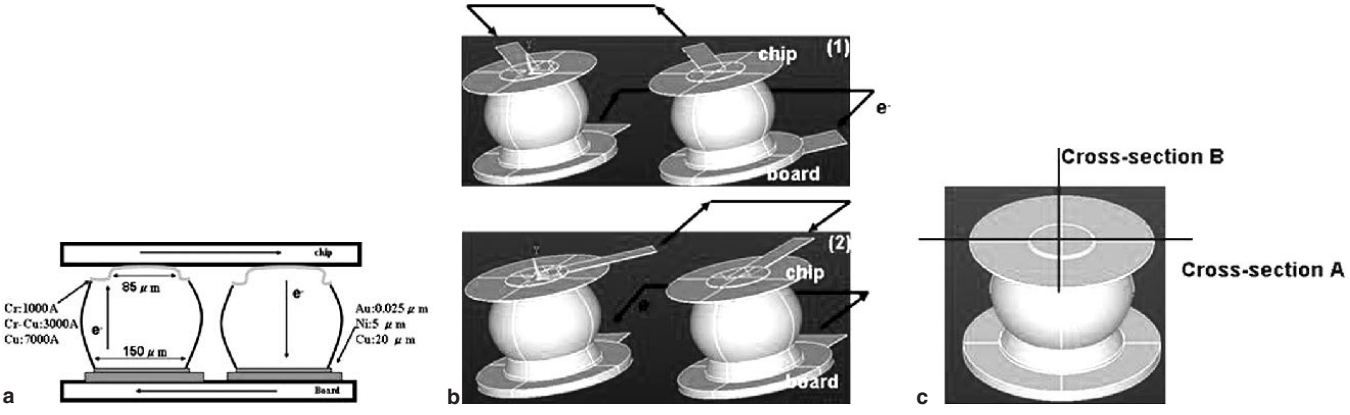

Fig. 2. (a) The schematic cross-sectional view of a pair of solder bumps. (b) The schematic three-dimensional view of the position of conducting lines related to the bumps: (1) Pair A and (2) Pair B. (c) The schematic three-dimensional view of a solder bump, defining cross-section plane A and cross-section plane B used in this study.

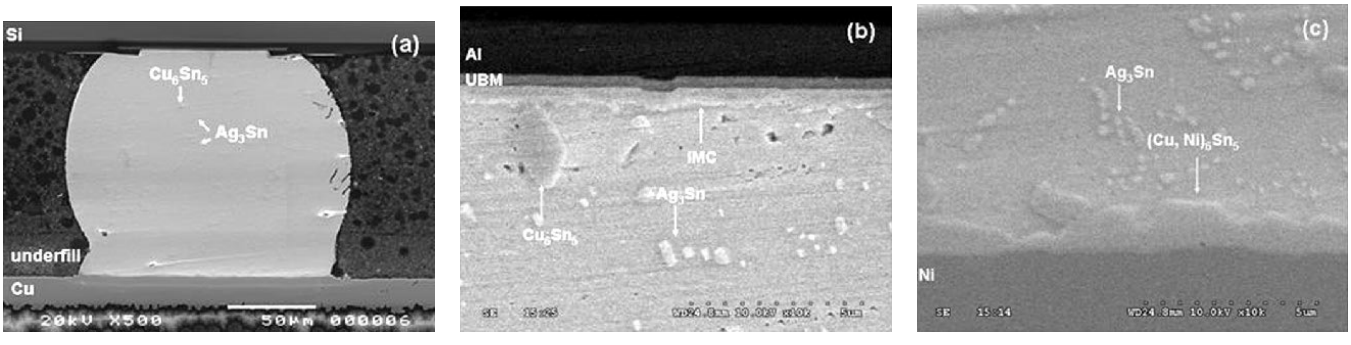

Fig. 3. The cross-sectional SEM images of a solder bump before current stressing: (a) whole bump view, (b) enlarged image on the chip side, and (c) enlarged image on the board side.

enlarged SEM images of the chip side and the BT board side, respectively. A layer of IMC with a thickness of 0.7 μm was formed between the solder and UBM interface at the chip side. On the BT board side, the IMC of Cu_6Sn_5 with dissolution of 15–20 at.% of Ni was observed.

Electromigration in the Cross-Sectioned Solder Bump

Figure 4a–d shows the microstructure evolution in the cross-sectioned SnAgCu bump before and after stressing by the current of 0.085 A for 20 h, 264 h, and 408 h at 100°C, respectively. The bump was polished in cross-section plane A before stressing, and the remaining cross-section area on the chip side was measured by the cross-sectional UBM length. Thus, the current density for the bump can be obtained. The current density used to stress the cross-sectioned bump is 2×10^4 A/cm^2. The direction of electron flow is from the chip side to the board side, as shown in the left bump of Pair A in Fig. 2b. Voids, formed at the solder and UBM interface after reflow, can be seen in Fig. 4a. After stressing for 20 h, a hillock was observed at the chip side, as indicated by the arrow in Fig. 4b. From EDS analysis, this hillock contained both Sn and Al. As shown in the left bump in Fig. 2b, the electrons enter the bump from the back left corner of the UBM on the chip side, migrating both Al and Sn atoms to form the hillock. After stressing for 264 h, no further damage was observed, as shown in Fig. 4c. However, after 408 h of stressing, the solder bump failed. In the upper left corner of the bump in Fig. 4d, a large void was observed, which may be responsible for the failure of the Pair A bump. Figure 5a shows the enlarged SEM images of the rectangular area in Fig. 4d. The surface of the void appears to be very smooth; from which, it may be inferred that the vicinity underwent a liquid state before failure occurred. Furthermore, some tiny solder balls were found on the surface near the void, which implies that the local temperature in the void may surpass the melting point of the solder at the moment of failure. Figure 5b shows the corresponding x-ray mapping for Al atoms. The migration of Al atoms can be clearly seen in the figure.

To examine the polarity effect, the current direction was reversed for the other bump of Pair A, i.e., the direction of electron flow goes from board side to chip side. Figure 6a–d shows the microstructure evolution before and after current stressing for 20 h, 264 h, and 408 h at 100°C, respectively. The Al was squeezed out at the chip/anode side after stressing. Figure 7a and b shows the enlarged SEM images of the damage and the corresponding x-ray mapping for Al at the interfacial region. On the board side, no obvious electromigration damage was found for the preceding two bumps. This may be attributed to the lower current density on the board side.

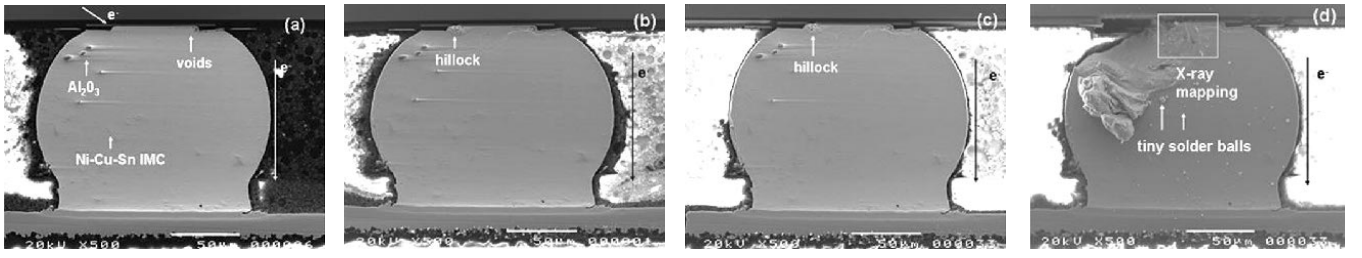

Fig. 4. The cross-sectional SEM images of the solder bump stressed at 100°C for (a) 0 h, (b) 20 h, (c) 264 h, and (d) 408 h.

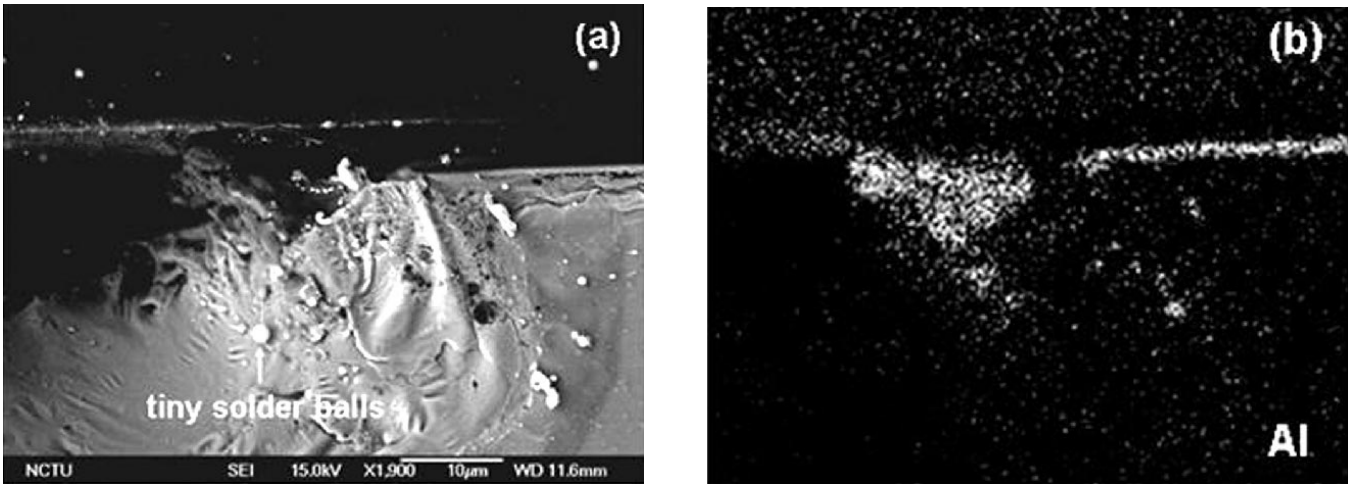

Fig. 5. (a) The enlarged SEM image of the rectangular area in Fig. 4d, and the corresponding x-ray mapping of (b) Al.

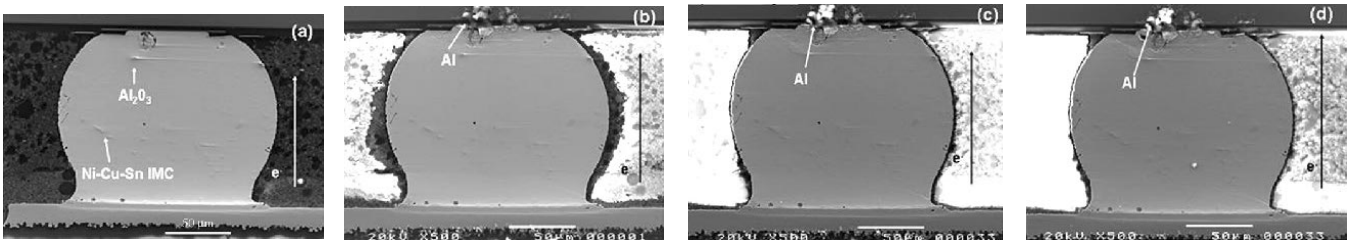

Fig. 6. The cross-sectional SEM images of the solder bump stressed at 100°C for (a) 0 h, (b) 20 h, (c) 264 h, and (d) 408 h.

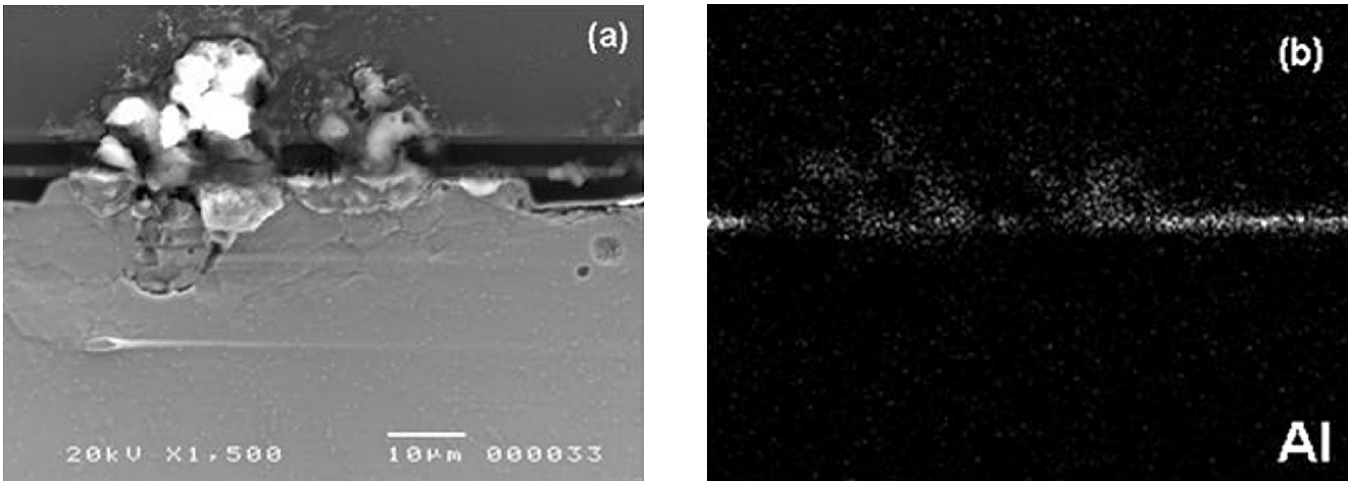

Fig. 7. (a) The magnified SEM image of the rectangular area in Fig. 6d and (b) are the x-ray elemental mapping for Al at interfacial region in (a).

Electromigration in Whole Bump

In the Pair B case, the set of whole bumps were stressed at the current density of 1×10^4 A/cm^2 until failure occurred. Afterwards, they were subject to cross sectioning for failure analysis. Figure 8a shows the cross-sectional SEM image of the solder bump along cross-section plane A. The bump failed after stressing for 140 h at 100°C and was then ground, cut, and polished away approximately 1/3 volume of the solder bump. The Cu-Sn IMCs were accumulated at the anode/board side, which implies that the copper atoms on the chip side and in the solder were caused to migrate by the electron flow to the board side.

To examine the microstructure beneath the cross-sectioned surface in Fig. 8a, further polishing was performed. Figure 8b and c shows the microstructures after polishing away half the volume and two-thirds the volume of the solder bump. Comparing both figures, cracks appear to be larger as the bump was polished down.

Figure 9 shows the cross-sectional SEM image of the solder bump along cross-sectioned plane B. The solder bump failed after 42 h of current stressing at 150°C. Because the test temperature was raised to 150°C, the failure time decreased from 140 h at 100°C to 42 h. Obviously, the voids at the right are much bigger than the ones on the left as the result of the current crowding effect.

DISCUSSION

Current Crowding Effect on Bump Failure

In the case of the cross-sectioned bump, the solder bump failed after 408 h of current stressing, as shown in Fig. 4a–d. The corresponding schematic picture of the bump is shown in the left bump of Pair A in Fig. 2b, where the electrons crowded into the bump from the upper left, back corner. At the early stage of current stressing, it was speculated that atoms around the corner migrated to the board/anode side, and voids started to form at the point where the current crowding occurred. As voids aggregated to form cracks, the contact area on the chip side decreased, forming a vicious cycle that deteriorated the contact. As the cracks moved toward the cross-sectioned surface, current density increased dramatically, heating up the bump locally because of joule heating. It is believed that the local temperature at the failure site was ramped over the melting point of the solder before failure because there were tiny solder balls observed near the voids. Furthermore, the surface morphology of the void has a smooth appearance, which also implies that the solder may have been in a molten state before the failure.

In Fig. 9, voids at the upper right corner are much bigger than those at the upper left corner. This may be the result of current crowding, where the electrons crowded into the bump from the upper right

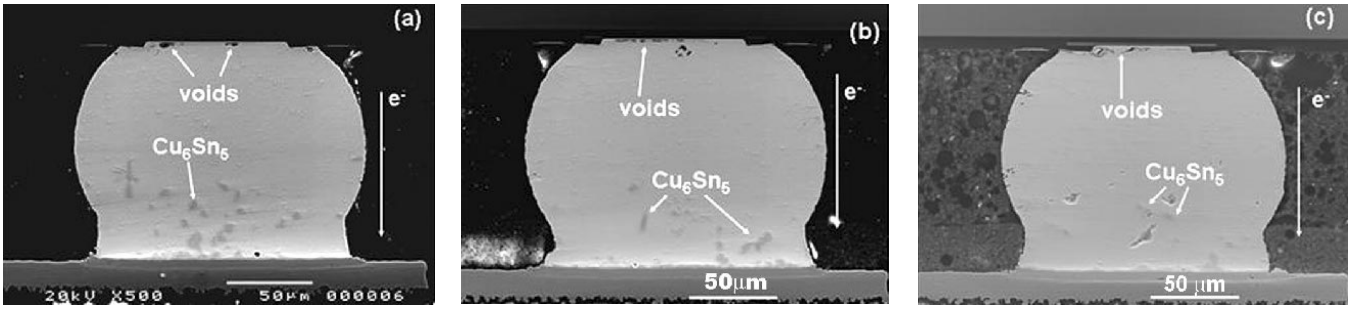

Fig. 8. The cross-sectional SEM image of the solder bump stressed at 100°C for 140 h: (a) after polishing to one-third of the bump volume, (b) after polishing half of the bump volume, and (c) after polishing two-thirds of the bump volume.

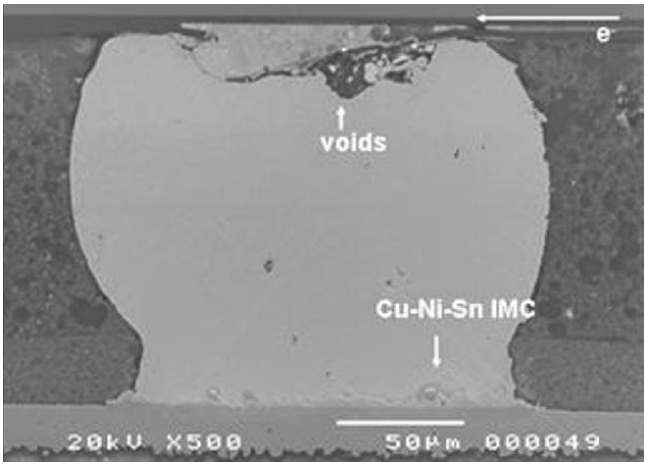

Fig. 9. The cross-sectional SEM image of the solder bump stressed at 150°C for 42 h.

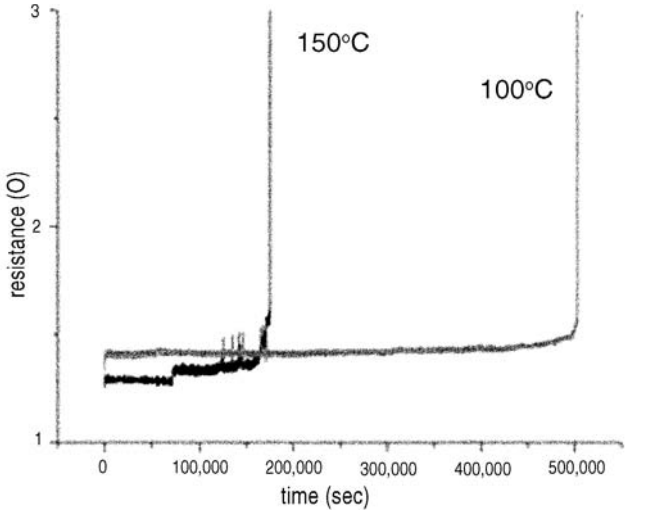

Fig. 10. The measured resistance of the stressing circuit as a function of stressing time.

corner of the bump. At the board side in Fig. 9, the Cu-Ni-Sn IMC grew thicker at the lower right corner, which was attributed to the current crowding on the board side.

Temperature Effect on Failure and Microstructure of the Bumps

The results for the measured resistance of the stressing circuit as a function of stressing time is shown in Fig. 10. Although the resistance included both the resistance of the conduction lines and that of the bump pair, it was still observed that the failure time depended on the dramatic increase of the resistance. As expected, the bump failed within 42 h of stressing time at 150°C and within 142 h at 100°C because the diffusivity of metal atoms are larger at high temperature. To examine the microstructure changes caused by the thermal effect, reference bumps were employed to undergo a similar thermal history during current stressing. Figure 11 shows the microstructure changes resulting from the thermal effect only. The bump was kept at 150°C for 42 h, and no obvious microstructure change was observed.

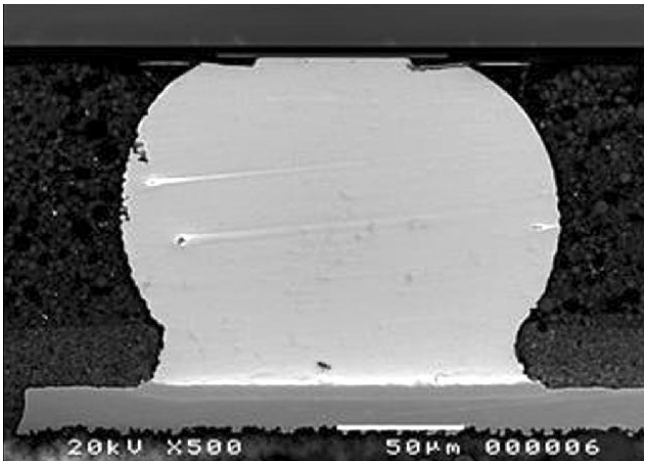

Fig. 11. The cross-sectional SEM image of the reference bump. The bump was kept at 150°C for 42 h.

Interface Analysis after Current Stressing

An enlarged image of the chip side of the bump in Fig. 8c is shown in Fig. 12. The crack was found at the solder/IMC interface. Above the crack, the EDS composition analysis at points 1 and 2 indicated that there were Al, Ti, Cr, Cu, and Sn in this region. It is believed that Al, Ti, and Cr atoms migrated by the electron flow into the IMC. Because Cu atoms were caused by the electron flow to migrate toward the board side to form a Sn-Cu compound, the analysis at points 3 and 4 revealed that only Sn and

Table I. The Composition of Solder at Points 1–4

	Point 1 (at. %)	Point 2 (at. %)	Point 3 (at. %)	Point 4 (at. %)
Al	11.66	9.04	not detected	not detected
Ti	5.54	4.19	not detected	not detected
Cr	14.41	16.47	not detected	not detected
Cu	14.00	14.65	not detected	not detected
Sn	54.39	55.74	98.39	98.15
Ag	not detected	not detected	1.61	1.85

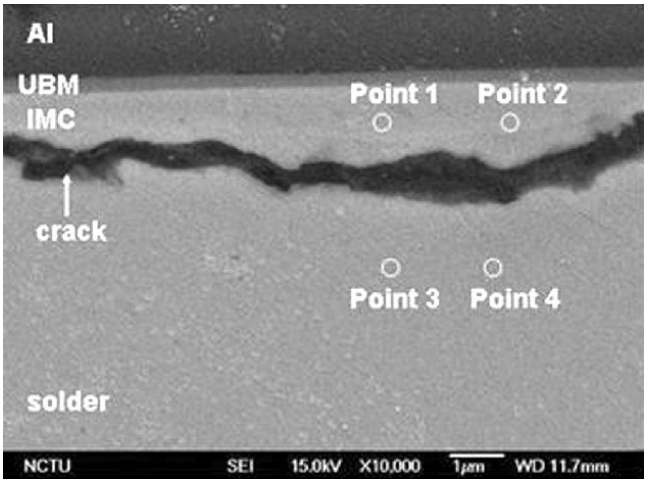

Fig. 12. The enlarged SEM image of the chip side in Fig. 8c

Ag atoms were detected at this region. The composition of these points in the solder is shown in Table I.

CONCLUSIONS

The electromigration-induced failures in SnAg3.8 Cu0.7 solder joints on Ti/Cr-Cu/Cu have been investigated under current density of 1×10^4 A/cm^2 and 2×10^4 A/cm^2 at 100°C and 150°C. The bumps failed at the chip/cathode side. Cracks occurred along the solder and UBM interface, which led to the open failure of the bump. The current crowding effect played an important role in the failure. However, the electron flow does not cause apparent damage at the board side because of a much lower current density there than that in the chip side.

ACKNOWLEDGEMENTS

The authors acknowledge the financial support of the National Science Council of Taiwan, Republic of China, through Grant No. NSC-90-2216-E-009-042; they are also grateful to Professor K.N. Tu, UCLA, for helpful discussions.

REFERENCES

1. K.N. Tu, J.W. Mayer, and L.C. Feldman, *Electronic Thin Film Science* (New York: Macmillan Publishing Company, 1992), p. 355.
2. J.H. Lau and S.-W.R. Lee, *Chip Scale Package* (New York: McGraw-Hill, 1999), p. 3.
3. H. Gan, W.J. Choi, G. Xu, and K.N. Tu, *JOM* 6, 34 (2002).
4. C.Y. Liu, C. Chen, and K.N. Tu, *J. Appl. Phys.* 88, 5703 (2000).
5. T.Y. Lee and K.N. Tu, *J. Appl. Phys.* 89, 3189 (2001).
6. K. Nakagawa, S. Baba, M. Watanabe, H. Matsushima, K. Harada, E. Hayashi, Q. Wu, A. Maeda, M. Nakanishi, and N. Ueda, *Electron. Comp. Technol. Conf.* (Piscataway, NJ: IEEE, 2001), pp. 917–977.
7. J.D. Wu, P.J. Zheng, K. Lee, C.T. Chiu, and J.J. Lee, *Electron. Comp. Technol. Conf.* (Piscataway, NJ: IEEE, 2002), pp. 452–457.
8. S.W. Chen, C.M. Chen, and W.C. Liu, *J. Electron. Mater.* 27, 1193 (1998).
9. C.M. Chen and S.W. Chen, *J. Electron. Mater.* 28, 902 (1999).
10. C.M. Chen and S.W. Chen, *J. Electron. Mater.* 29, 1222 (2000).
11. C.M. Chen and S.W. Chen, *J. Appl. Phys.* 90, 1208 (2001).
12. S.Y. Jang, J. Wolf, W.S. Kwon, and K.W. Paik, *Electron. Comp. Technol. Conf.* (Piscataway, NJ: IEEE, 2002), pp. 1213–1220.
13. T.Y. Lee and K.N. Tu, *J. Appl. Phys.* 90, 4502 (2001).
14. H. Gan and K.N. Tu, *Electron. Comp. Technol. Conf.* (Piscataway, NJ: IEEE, 2002), pp. 1206–1212.
15. K.N. Tu, C.C. Yeh, C.Y. Liu, and C. Chen, *Appl. Phys. Lett.* 76, 988 (2000).
16. T.Y.T. Lee, T.Y. Lee, and K.N. Tu, *Electron. Comp. Technol. Conf.* (Piscataway, NJ: IEEE, 2001), pp. 558–563.
17. E.C.C. Yeh and K.N. Tu, *J. Appl. Phys.* 89, 3203 (2001).
18. E.C.C. Yeh, W.J. Choi, and K.N. Tu, *Appl. Phys. Lett.* 80, 580 (2002).
19. W.J. Choi, E.C.C. Yeh, and K.N. Tu, ECTC, *Electron. Comp. Technol. Conf.* (Piscataway, NJ: IEEE, 2002), pp. 1201–1205.